The Journal of Immunology

RESEARCH ARTICLE | NOVEMBER 15 2008

Macrophage Antigen Complex-1 Mediates Reactive Microgliosis and Progressive Dopaminergic Neurodegeneration in the MPTP Model of Parkinson's Disease[1] FREE

Xiaoming Hu; ... et. al

J Immunol (2008) 181 (10): 7194–7204.
https://doi.org/10.4049/jimmunol.181.10.7194

Macrophage Antigen Complex-1 Mediates Reactive Microgliosis and Progressive Dopaminergic Neurodegeneration in the MPTP Model of Parkinson's Disease[1]

Xiaoming Hu,* Dan Zhang,* Hao Pang,* W. Michael Caudle,† Yachen Li,* Huiming Gao,* Yuxin Liu,* Li Qian,* Belinda Wilson,* Donato A. Di Monte,‡ Syed F. Ali,§ Jing Zhang,† Michelle L. Block,*¶ and Jau-Shyong Hong[2]*

Neuronal death is known to trigger reactive microgliosis. However, little is known regarding the manner by which microglia are activated by injured neurons and how microgliosis participates in neurodegeneration. In this study we delineate the critical role of macrophage Ag complex-1 (MAC1), a member of the β_2 integrin family, in mediating reactive microgliosis and promoting dopaminergic (DAergic) neurodegeneration in the 1-methyl-4-phenyl-1,2,3,6-tetrahydropyridine (MPTP) model of Parkinson's disease. MAC1 deficiency greatly attenuated the DAergic neurodegeneration induced by MPTP or 1-methyl-4-phenyl-pyridium iodide (MPP^+) exposure both in vivo and in vitro, respectively. Reconstituted experiments created by adding microglia from $MAC1^{-/-}$ or $MAC1^{+/+}$ mice back to $MAC1^{+/+}$ neuron-enriched cultures showed that microglia with functional MAC1 expression was mandatory for microglia-enhanced neurotoxicity. Both in vivo and in vitro morphological and Western blot studies demonstrated that MPTP/MPP^+ produced less microglia activation in $MAC1^{-/-}$ mice than $MAC1^{+/+}$ mice. Further mechanistic studies revealed that a MPP^+-mediated increase in superoxide production was reduced in $MAC1^{-/-}$ neuron-glia cultures compared with $MAC1^{+/+}$ cultures. The stunted production of superoxide in $MAC1^{-/-}$ microglia is likely linked to the lack of translocation of the cytosolic NADPH oxidase (PHOX) subunit ($p47^{phox}$) to the membrane. In addition, the production of PGE_2 markedly decreased in neuron plus $MAC1^{-/-}$ microglia cocultures vs neuron plus $MAC1^{+/+}$ microglia cocultures. Taken together, these results demonstrate that MAC1 plays a critical role in MPTP/MPP^+-induced reactive microgliosis and further support the hypothesis that reactive microgliosis is an essential step in the self-perpetuating cycle leading to progressive DAergic neurodegeneration observed in Parkinson's disease. *The Journal of Immunology,* **2008, 181: 7194–7204.**

Parkinson's disease (PD)[3] is a progressively disabling neurodegenerative disorder affecting >1.5 million people in the United States. It is characterized by the loss of dopaminergic (DAergic) neurons in the substantia nigra pars compacta (SNpc) and the consequent loss of dopamine (DA) in the striatum, resulting in locomotor impairments including slowness in spontaneous movement, resting tremor, and rigidity (1). Unfortunately, an ideal therapy without long-term debilitating side effects is not available for PD patients. The development of effective neuroprotective therapies needs collective efforts to elucidate the mechanisms underlying the progressive degeneration of DA-containing neurons in PD.

Microglia are the primary immune effector cells resident within the CNS (2). The microglial response secondary to direct neuronal lesions is usually termed reactive microgliosis, a process involving increased proliferation, recruitment, and activation of microglia (3). Reactive microgliosis has been observed in PD (4) and a variety of other neurodegenerative diseases (5) or CNS injury (6). Microglial activation functions in a neuroprotective manner in the CNS by scavenging excess neurotoxins, removing dying cells and cellular debris (7), and stimulating repair processes after brain damage (8, 9). Overactivated microglia, however, exert cytotoxic effects which, in turn, enhance the neuronal damage by producing and releasing a plethora of neurotoxic substances that include free radicals and proinflammatory cytokines (10). Hence, a vicious cycle may develop between neuronal degeneration and reactive microgliosis and take an active role in the progressive nature of DAergic neurodegeneration in PD (11).

The importance of reactive microgliosis in the progress of PD has been best characterized with the 1-methyl-4-phenyl-1,2,3,6-tetrahydropyridine (MPTP) model. MPTP is converted to the 1-methyl-4-phenyl-2,3-dihydropyridium ion (MPP^+) in astrocytes and causes selective DAergic neuronal loss in the SNpc, leading to a severe parkinsonian syndrome (12, 13). Persistent microglial activation has been detected in the SNpc of humans

*Neuropharmacology Section, Laboratory of Pharmacology and Chemistry, National Institute of Environmental Health Sciences, Research Triangle Park, NC 27709; †Department of Pathology, University of Washington, Seattle, WA 98104; ‡The Parkinson's Institute, Sunnyvale, CA 940852; §Neurochemistry Laboratory, National Center for Toxicological Research/Food and Drug Administration, Jefferson, AR 72079; and ¶Department of Anatomy and Neurobiology, Virginia Commonwealth University Medical Campus, Richmond, VA 23298

Received for publication June 2, 2008. Accepted for publication September 8, 2008.

The costs of publication of this article were defrayed in part by the payment of page charges. This article must therefore be hereby marked *advertisement* in accordance with 18 U.S.C. Section 1734 solely to indicate this fact.

[1] This work was supported by the Intramural Research Program of the National Institutes of Health, National Institute of Environmental Health Sciences. M.L.B. was supported by the National Institutes of Health Pathway to Independence Award (NIEHS 1K99ES01549-01).

[2] Address correspondence and reprint requests to Dr. Jau-Shyong Hong, Mail Drop F1-01 National Institute of Environmental Health Sciences, P.O. Box 12233, Research Triangle Park, NC 27709. E-mail address: hong3@niehs.nih.gov

[3] Abbreviations used in this paper: PD, Parkinson's disease; DAergic, dopaminergic; DOPAC, 3,4-dihydroxyphenylacetic acid; HVA, homovanillic acid; MAC1, macrophage antigen complex-1; MPTP, 1-methyl-4-phenyl-1,2,3,6-tetrahydropyridine; MPP^+, 1-methyl-4-phenyl-pyridium iodide; PHOX, NADPH oxidase; SNpc, substantia nigra pars compacta; SOD, superoxide dismutase; TH, tyrosine hydroxylase; DA, dopamine; ECM, extracellular matrix.

(14) and nonhuman primates (15) years after initial MPTP exposure. Additionally, administration of MPTP to mice led to robust gliosis in the SNpc and the striatum (16). This activation of microglia preceded abundant DAergic neurodegeneration in the SNpc (17), suggesting that microgliosis may contribute to DAergic cell loss. Furthermore, blockade of microglial activation with minocycline prevents nigrostriatal DAergic neurodegeneration induced by MPTP in a mouse model of PD (18). Finally, the presence of microglia appears to exacerbate MPP^+-mediated DAergic toxicity in neuronal cultures (19). These reports highlight the importance of microglial activation in MPTP-induced DAergic neurodegeneration. However, little is known regarding the manner by which injured neurons elicit microgliosis and how microgliosis participates in DAergic neurodegeneration. Therefore, the identification of a microglial surface receptor that may mediate reactive microgliosis is of great interest in elucidating the mechanisms of PD progression and developing therapeutic strategies.

Recent evidence indicated that macrophage Ag complex-1 (MAC1; CR3, CD11b/CD18, $\alpha_M\beta_2$) may be involved in mediating the activation of microglia in inflammatory demyelinating disease (20). MAC1 is a member of the leukocyte-specific β_2 integrin family. It is both an adhesion molecule and a pattern recognition receptor, and has long been recognized to orchestrate the inflammatory response by regulating diverse functions involved in adhesion, migration, phagocytosis, and chemotaxis (21). Additionally, MAC1 has been documented to play an important role in NADPH oxidase (PHOX) activation in response to oxidative insults (22–24). Other evidence suggests that MAC1 occupancy is capable of triggering the transcription factor NF-κB signaling pathway and the subsequent production of inflammatory factors (25, 26).

It has been reported in animal experiments and postmortem human studies that the increase in MAC1 expression corresponds to microglial activation in numerous neurodegenerative diseases, including PD (16, 27). However, the biological significance of this increased expression to neurodegeneration remains unclear. Thus, in the present study we delineate the contribution of MAC1 to DAergic neurodegeneration in both in vivo and in vitro models of PD. We also present evidence for the importance of MAC1 in mediating microgliosis and the microglia-induced oxidative stress and inflammatory response.

Materials and Methods

Reagents

MPTP and MPP^+ were purchased from Sigma-Aldrich. LPS (strain O111:B4) was purchased from Calbiochem. WST-1 was purchased from Dojindo Laboratories. Cell culture ingredients were obtained from Invitrogen. [^{3}H]DA (30 Ci/mmol) was purchased from PerkinElmer Life Sciences. The polyclonal Ab to tyrosine hydroxylase (TH) was donated by Dr. J. Reinhard of GlaxoSmithKline. mAb to F4/80 was obtained from Serotec. Polyclonal Ab to Iba1 was obtained from Wako Chemicals. Rabbit anti-p47^{phox} was obtained from Upstate Biotechnology. Rabbit anti-GAPDH was obtained from Abcam. Mouse anti-gp91^{phox} was purchased from BD Transduction Laboratories. Vectastain avidin-biotinylated enzyme complex and biotinylated horse anti-mouse and goat anti-rabbit secondary Abs were purchased from Vector Laboratories. FITC-conjugated goat anti-rabbit IgG was obtained from Jackson ImmunoResearch Laboratories. PGE_2 EIA kit was purchased from Cayman Chemical.

Animals

B6.129S4-Itgam^{tm1Myd}/J ($MAC1^{-/-}$, on a C57BL/6J background) and C57BL/6J ($MAC1^{+/+}$) mice were purchased from The Jackson Laboratory. All the animals were housed in a specific pathogen-free facility and fed a standard laboratory chow ad libitum. Housing, breeding, and experimental use of the animals were performed in strict accordance with the National Institutes of Health guidelines.

Primary midbrain neuron-glia cultures

Primary midbrain neuron-glia cultures were prepared from the brains of embryonic day 13 ± 0.5 $MAC1^{+/+}$ and $MAC1^{-/-}$ mice as previously described (19). In brief, the ventral midbrain portion of the embryonic brains was dissected out under a microscope and kept in cold MEM. Mesencephalic tissues were isolated and dissociated with gentle mechanical trituration. Cells were diluted to 1.5×10^6/ml in maintenance medium (MEM supplemented with 10% heat-inactivated FBS, 10% heat-inactivated horse serum, 1 g/L glucose, 2 mM L-glutamine, 1 mM sodium pyruvate, 100 μM nonessential amino acids, 50 U/ml penicillin, and 50 μg/ml streptomycin) and seeded in 24-well culture plates precoated with poly-D-lysine (20 μg/ml). Plates were maintained at 37°C in a humidified atmosphere of 5% CO_2 and 95% air. Seven-day-old cultures were used for treatment. The composition of the cells at the time of treatment was ~48% astrocytes, 12% microglia, and 40% neurons with 1% of the neurons being TH-positive neurons.

Primary midbrain neuron-enriched cultures

Cytosine β-D-arabinofuranoside (Ara-C) was added to a final concentration of 6 μM 36 h after seeding the cells to suppress glial proliferation. Cultures were changed back to maintenance medium 2 days later and were used for treatment 7 days after initial seeding.

Primary microglia-enriched cultures

Primary microglia-enriched cultures were prepared from the whole brains of 1-day-old $MAC1^{+/+}$ and $MAC1^{-/-}$ pups as described previously (19). In brief, brain tissues were triturated after removing the meninges and blood vessels. Cells were seeded at 5×10^7 in 150-cm^3 culture flasks with DMEM/F12 containing 10% heat-inactivated FBS, 2 mM L-glutamine, 1 mM sodium pyruvate, 100μM nonessential amino acids, 50 U/ml penicillin, and 50 μg/ml streptomycin. After a confluent monolayer of glial cells had been obtained (12–14 days after initial seeding) microglia were shaken off, collected, and seeded.

Neuron-microglia cocultures

Enriched microglia (1×10^5/well) from $MAC1^{+/+}$ or $MAC1^{-/-}$ mice were seeded to 6-day-old neuron-enriched cultures from $MAC1^{+/+}$ mice. Reconstituted cultures were used for MPP^+ treatment the following day. Neurotoxicity was analyzed 7 days after the treatment.

Uptake assay

Uptake of [^{3}H]DA was performed as previously described (28). In brief, cultures were incubated for 20 min at 37°C with 1 μM [^{3}H]DA in Krebs-Ringer buffer (16 mM sodium phosphate, 119 mM NaCl, 4.7 mM KCl, 1.8 mM $CaCl_2$, 1.2 mM $MgSO_4$, 1.3 mM EDTA, and 5.6 mM glucose; (pH 7.4)). Nonspecific DA uptake was blocked with mazindol (10 μM). Cells were collected in 1N NaOH after washing with ice-cold Krebs-Ringer buffer. Radioactivity was determined by liquid scintillation counting with a Beckman Tri-Carb 2900TR liquid scintillation counter. Specific [^{3}H]DA uptake was calculated by subtracting the mazindol counts from the wells without the uptake inhibitor.

MPTP injection

For 6 consecutive days, 8-wk-old male mice received daily MPTP injections (15 mg/kg of MPTP · HCl (14.52 mg/kg as a base), s.c.). Mice used as controls received an equal volume of 0.9% saline. The mice were euthanized 21 days after the last MPTP/saline treatment with an i.p. injection of 120 mg/kg pentobarbital and then perfused through the left ventricle with saline followed by 4% paraformaldehyde. Brains were removed and postfixed in 4% paraformaldehyde overnight at 4°C. Brains were then placed into 30% sucrose/PBS solution at 4°C until the brains sank to the bottom of the container. Coronal sections including SNpc were cut on a horizontal sliding microtome into 35-μm transverse free-floating sections.

Immunostaining

Immunostaining was performed as described previously (29). DAergic neurons were stained with the Ab to TH (1/5000). Microglia were stained with the Ab raised against F4/80 (1/20) or Iba1 (1/1000). In brief, brain sections or 3.7% formaldehyde-fixed cultures were treated with 1% hydrogen peroxide followed by sequential incubation with blocking solution (PBS containing 1% BSA, 0.4% Triton X-100, and 4% appropriate serum), primary Ab, biotinylated secondary Ab, and Vectastain ABC reagents. After washing, the bound complex was visualized by incubating with 3, 3′-diaminobenzidine and urea-hydrogen peroxide tablets dissolved in water.

Color development was terminated by removal of the reagents and washing with PBS. Images of in vitro cultures or brain staining were recorded with an inverted microscope (Nikon) or Zeiss microscope, respectively, connected to a charge-coupled device camera (DAGE-MTI) operated with the MetaMorph software (Molecular Devices).

Cell counting

For visual enumeration of the immunostained TH-positive neurons in the cell cultures, all cells in a well of a 24-well-plate were counted under the microscope at ×100 magnification. For in vivo quantification of TH-positive neurons, 24 consecutive brain slices (35-μm thickness), which encompass the entire SNpc, were collected. The first (rostral) and every fourth section of the 24 sections of each brain (i.e., eight evenly spaced sections/brain) from saline or MPTP-injected animals were used for the cell counting. The number of TH-positive neurons in the SNpc region was counted in a double-blind manner by applying unbiased stereological analysis as previously described (30, 31). In brief, the total number of TH-positive neurons was counted using the optical fractionator method, and the SNpc was delineated using previously described criteria (32, 33). After delineation at low magnification, every fourth section was sampled at higher magnification using the Cast grid system (Olympus).

Analysis of striatal catecholamine content

The levels of DA and its metabolites (3,4-dihydroxyphenylacetic acid (DOPAC) and homovanillic acid (HVA)) were determined by HPLC and coupled with electrochemical detection as described (34). In brief, striatal tissues were sonicated in 0.2 M perchloric acid (20% w/v) containing the internal standard 3,4-dihydroxybenzylamine (100 ng/ml). After centrifugation, 150 μl of the supernatant was passed through a 0.2-μm Nylon-66 filter, and 25 μl of the filtrate representing 2.5 mg of striatal tissue was used. The concentrations of DA, DOPAC, and HVA were calculated using standard curves that were generated by determining, in triplicate, the ratios between three known amounts of the internal standard.

MPP^+ measurement

$MAC1^{+/+}$ and $MAC1^{-/-}$ mice were injected with a single dose of 40 mg/kg MPTP s.c. and sacrificed 90 min later. Both (left and right) striata were dissected on ice, placed into a vial containing 250 μl of 0.4 N perchloric acid, and sonicated. After centrifugation, MPP^+ was measured by HPLC using a Selectosil 5 SCX column (Phenomenex). The mobile phase was delivered at a flow rate of 1.0 ml/min and consisted of 90% of a mixture of 0.1 M acetic acid and 0.15 M triethylamine hydrochloride (adjusted to pH 2.3 with formic acid) and 10% acetonitrile.

Superoxide assay

The extracellular superoxide production was determined by measuring the superoxide dismutase (SOD)-inhibitable reduction of tetrazolium salt, WST-1, as described before (28) with modifications. Seven-day-old primary neuron-glia cultures grown in 96-well plates were treated with MPP^+ or vehicle in 150 μl of phenol red-free treatment medium. At 4 or 7 days after treatment, 50 μl of WST-1 (1 mM) in phenol red-free treatment medium, with or without SOD (600 U/ml), was added. The absorbance at 450 nm was read immediately with a Spectra Max Plus microtiter plate spectrophotometer (Molecular Devices). For the superoxide assay using microglia-enriched culture, cells were plated at 1×10^5/well in 96-well plates and incubated for 12 h. The cells were washed twice and left in 100 μl of HBSS. Fifty μl of HBSS, PMA, MPP^+, or LPS was added. Then 50 μl of WST-1 (1 mM) in HBSS, with or without SOD (600 U/ml), was added. The absorbance at 450 nm was read immediately.

Confocal microscopy

Enriched microglial cells from mice were seeded in dishes at 5×10^4 cells/well and treated with LPS for 10 min. Cells were fixed with 3.7% paraformaldehyde in PBS for 10 min. After washing with PBS, cells were incubated with rabbit polyclonal Ab to $p47^{phox}$ (0.5 μg/ml). Cells were then washed and incubated with FITC-conjugated goat anti-rabbit Ab. Focal planes spaced at 0.4-μm intervals were imaged with a Zeiss 510 laser scanning confocal microscope (63X PlanApo 1.4 numerical aperture objective) equipped with LSM510 digital imaging software.

Cell extracts

Whole cell lysis from neuron-glia cultures were prepared with lysis buffer (Cell Signaling Technology). Subcellular fractionation was performed as described previously (35). For subcellular fractions, microglia were lysed in hypotonic lysis buffer (1 mM EGTA, 1 mM EDTA, 10 mM β-glycerophosphate, 10 mM NaF, 1 mM sodium orthovanadate, 2 mM $MgCl_2$, 10 mM DTT, 1 mM PMSF, and 10 μg/ml each of leupeptin, aprotinin, and pepstatin A), incubated on ice for 30 min, and then subjected to Dounce homogenization (20–25 stokes, tight pestle A). The lysates were loaded onto a sucrose gradient in lysis buffer (final 0.5 M) and centrifuged at $1600 \times g$ for 15 min. The supernatant above the sucrose gradient was used as the cytosolic fraction after centrifugation at $150{,}000 \times g$ for 30 min. The pellet was solubilized in 1% Nonidet P-40 hypotonic lysis buffer and was used as the membranous fraction.

Tissue extracts

The midbrain encompassing the SN was removed from saline perfused mice and homogenized in lysis buffer (PBS containing 1% Nonidet P-40 and a mixture of protease inhibitors). After 30 min on ice, the homogenate was centrifuged to remove the insoluble fraction.

Western blot analysis

Equal amount of protein (60 μg/lane) was separated by 4–12% Bis-Tris-polyacrylamide electrophoresis gel and transferred to polyvinylidene difluoride membranes (NOVEX). The membranes were blocked with 5% nonfat milk and incubated with primary Ab (rabbit anti-$p47^{phox}$ Ab (1/2000), rabbit anti-GAPDH (1/2000), mouse anti-$gp91^{phox}$ (1/2000), or rabbit anti-Iba1 (1/3000) overnight at 4°C. The membranes were then incubated with HRP-linked anti-rabbit or mouse IgG (1/3000) for 1 h at 25°C. ECL Plus reagents (GE Healthcare) were used as a detection system.

PGE_2 production assay

Cultures in 24-well plates were treated with MPP^+. Supernatant was collected 4 days later, and PGE_2 production in supernatant was determined with a PGE_2 EIA kit according to the manufacturer's instructions.

Statistical analysis

The data were expressed as mean ± SEM. Statistical significance between two groups was assessed with an ANOVA followed by Student's t test. Statistical significance between multiple groups was performed using a one- or two-way ANOVA. When ANOVA showed a significant difference, a least significant difference multiple comparisons posthoc test was performed. A value of $p < 0.05$ was considered statistically significant.

Results

MPP^+-induced DAergic neurotoxicity in neuron-glia cultures was attenuated in the absence of MAC1

To investigate the role of MAC1 in MPTP/MPP^+-induced neurotoxicity, neuron-glia cultures prepared from $MAC1^{+/+}$ and $MAC1^{-/-}$ mice were treated with either a vehicle or different concentrations of MPP^+ (0.125, 0.25, or 0.5 μM). MPP^+ instead of MPTP was used in all in vitro experiments because MPTP is not toxic to astrocyte-devoid cultures, such as neuron-enriched and neuron-microglia cocultures, which were frequently used in the present study. Moreover, a previous report from our laboratory has demonstrated that MPTP and MPP^+ are equally potent to induce DAergic neuron degeneration in our culture systems (19).

DAergic neurotoxicity was assessed by the number and morphological analysis of DAergic neurons and by the [^{3}H]DA uptake assay. TH, the rate-limiting enzyme in the synthesis of DA, is used as a marker of DAergic neurons. DA uptake assay measures the capacity of DAergic neurons to take up ^{3}H-labeled DA, which is a functional index of DAergic neurons. Morphological analysis after immunocytochemistry staining with an anti-TH Ab showed that TH-positive neurons in the MPP^+-treated $MAC1^{+/+}$ cultures (Fig. 1*A*) displayed much shorter and less elaborate TH-positive processes compared with those from $MAC1^{-/-}$ cultures. Concentration-dependent decreases in the number of TH-positive neurons (Fig. 1*B*) and [^{3}H]DA uptake capacity (Fig. 1*C*) were observed in cultures from both $MAC1^{+/+}$ and $MAC1^{-/-}$ mice. The reduction observed for both of these measurements was much less in $MAC1^{-/-}$ compared with $MAC1^{+/+}$ cultures.

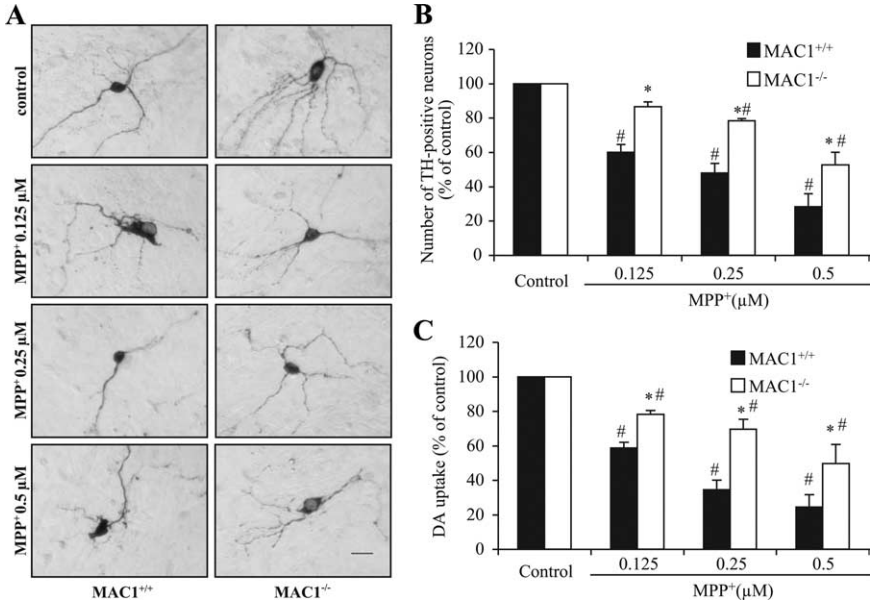

FIGURE 1. MPP^+-induced DAergic neurotoxicity was attenuated in mesencephalic neuron-glia cultures from $MAC1^{-/-}$ mice compared with $MAC1^{+/+}$ mice. Mouse ($MAC1^{+/+}$ and $MAC1^{-/-}$) mesencephalic neuron-glia cultures in 24-well plates were treated with vehicle or different concentration of MPP^+ (0.125 μM, 0.25 μM and 0.5 μM) for 7 days. *A*, Representative microscopic images were shown for TH-positive neurons treated with vehicle or different concentrations of MPP^+. Scale bar: 30 μm. *B*, The effect of MPP^+ on the number of DAergic neurons was assessed by counting the number of TH-positive cells remaining in the neuron-glia cultures after vehicle or MPP^+ treatments. *C*, MPP^+-induced DAergic neurotoxicity was quantified by the [^{3}H]DA uptake assay, which measures the capacity of DAergic neurons to take up ^{3}H-labeled DA. Results were expressed as a percentage of the vehicle-treated controls and were the mean ± SEM from four independent experiments in duplicate. #, $p < 0.05$ compared with corresponding vehicle-treated controls. ∗, $p < 0.05$ compared with $MAC1^{+/+}$ cultures after same treatments.

Microglia are essential for MAC1-potentiated neurotoxicity of MPP^+

It is well documented that MPTP/MPP^+ causes direct damage to DAergic neurons. Additionally, microglia have been shown to play an active role in exacerbating MPTP/MPP^+-induced DAergic neuronal loss (19). To ensure that the effect of MAC1 on the course of MPP^+-induced neurotoxicity was not a consequence of developmental alterations and dampened sensitivity of DAergic neurons in $MAC1^{-/-}$ animals, we compared the MPP^+-induced neurotoxicity in neuron-enriched cultures from $MAC1^{+/+}$ and $MAC1^{-/-}$ mice. The number of DAergic cells was reduced to similar levels in $MAC1^{+/+}$ and $MAC1^{-/-}$ neuron-enriched cultures after MPP^+

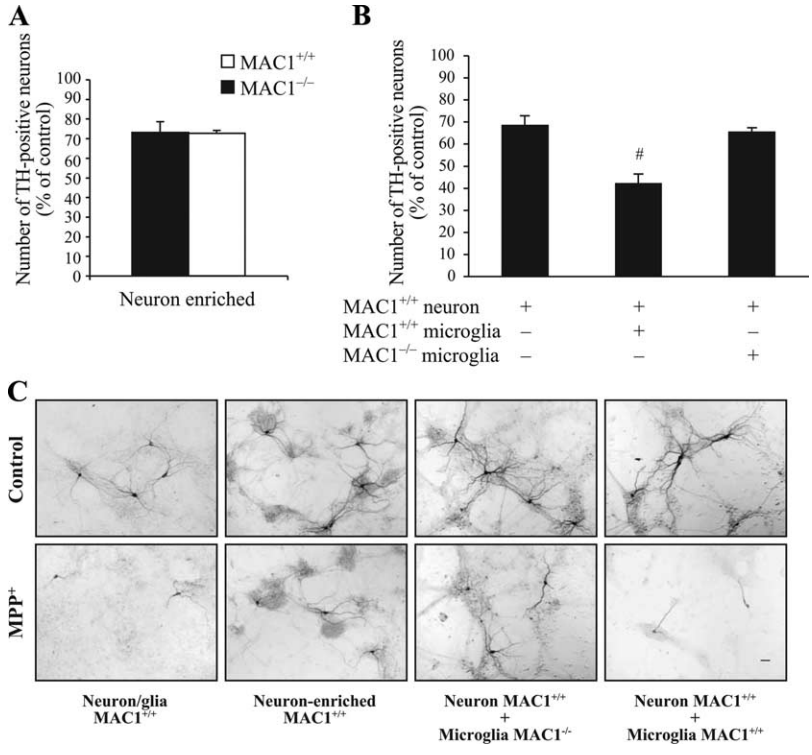

FIGURE 2. Expression of MAC1 on microglia is important for MPP^+-induced neurotoxicity. *A*, Mesencephalic neuron-enriched cultures from $MAC1^{+/+}$ or $MAC1^{-/-}$ mice were compared for their susceptibility to MPP^+-induced DAergic neurotoxicity. *B*, Neuron-enriched cultures from $MAC1^{+/+}$ mice with microglia ($MAC1^{+/+}$ or $MAC1^{-/-}$) added back were compared for their susceptibility to MPP^+-induced neurotoxicity. Microglia (1×10^5/well) were added back to neuron-enriched cultures 24 h before treatment. Cultures were treated with vehicle or 0.25 μM MPP^+ for 7 days, and MPP^+-induced neurotoxicity was quantified by counting TH-positive neurons. The data were expressed as the percentage of corresponding vehicle-treated control cultures and were the mean ± SEM from three independent experiments in triplicate. #, $p < 0.05$ relative to neuron-enriched cultures with or without $MAC1^{-/-}$ microglia added back. *C*, Representative microscopic images were shown for TH-positive neurons treated with vehicle or MPP^+. Scale bar: 50 μm.

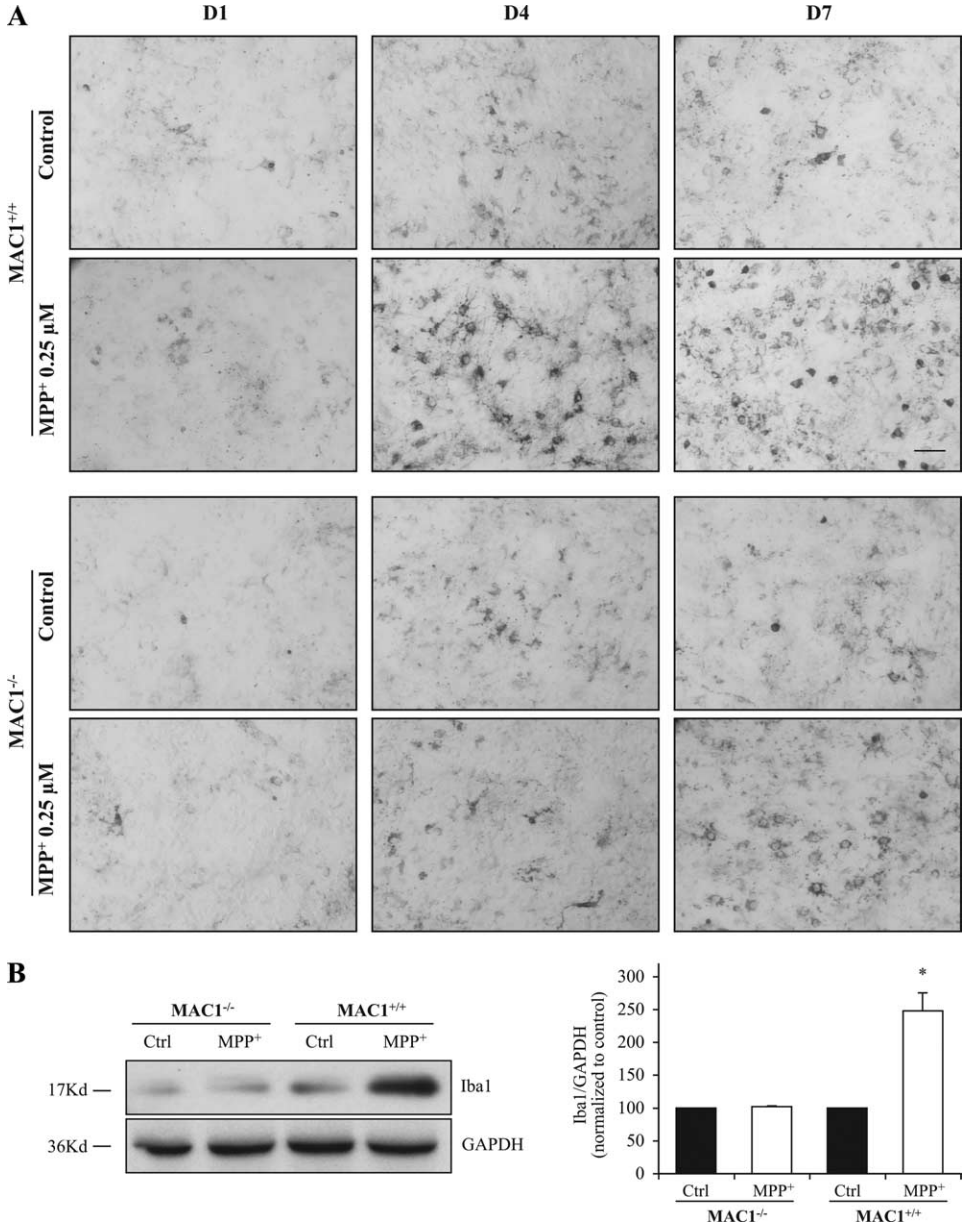

FIGURE 3. Analysis of MPP^+-induced reactive microgliosis in vitro. Mesencephalic neuron-glia cultures from $MAC1^{+/+}$ and $MAC1^{-/-}$ mice were treated with vehicle or MPP^+ (0.25 μM). *A*, Cultures were fixed at 1, 4, and 7 days (D) after treatments. Microglia was visualized by immunostaining of the F4/80 Ag, a microglia marker. The images presented are representative of three independent experiments. Scale bar: 50 μm. *B*, Western blot analysis of microglial activation. Cell lysates of cultures from $MAC1^{+/+}$ and $MAC1^{-/-}$ mice were prepared 4 days after MPP^+ treatment. Immunoblot analysis was performed to assess Iba1 Ag. GAPDH was used as loading control (Ctrl). The ratio of densitometry values of Iba1 and GAPDH was analyzed and normalized to each respective control. The experiment has been performed three times. Results were presented as the mean ± SEM. $*$, $p < 0.05$ relative to corresponding vehicle-treated control cultures.

treatment (Fig. 2*A*), suggesting that DAergic neurons from $MAC1^{+/+}$ and $MAC1^{-/-}$ mice respond equally to MPP^+ exposure in the absence of glia cells. It is noteworthy that greater neuronal loss was detected in $MAC1^{+/+}$ neuron-glia cultures (52% loss; Fig. 1*B*) than in $MAC1^{+/+}$ neuron-enriched cultures (30% loss; Fig. 2*A*) following the same concentration (0.25 μM) of MPP^+ treatment. However, this glia-enhanced MPP^+ neurotoxicity was not observed in neuron-glia cultures from $MAC1^{-/-}$ mice, emphasizing the importance of glia in MAC1-potentiated MPP^+ neurotoxicity. Further evidence of the importance of microglial MAC1 expression was demonstrated by the difference between the number of DAergic neurons detected when microglia from $MAC1^{+/+}$ or $MAC1^{-/-}$ mice were added to $MAC1^{+/+}$ neuron-enriched cultures before MPP^+ treatment (Fig. 2*B*). The addition of $MAC1^{+/+}$ microglia resulted in ~20% exacerbation of DAergic neuronal loss, which is similar to the degree of reduction observed in $MAC1^{+/+}$ neuron-glia cultures vs neuron-enriched cultures. The addition of $MAC1^{-/-}$ microglia, however, failed to show more neurotoxicity compared with $MAC1^{+/+}$ neuron-enriched cultures. The morphological changes elicited in TH-positive neurons in $MAC1^{+/+}$ neuron-glia culture, neuron-enriched cultures, and neuron-enriched cultures supplemented with microglia from $MAC1^{+/+}$ or $MAC1^{-/-}$ mice were shown in Fig. 2*C*. Taken together, these data confirm that the function of MAC1 in the severity of MPP^+-mediated DAergic neurotoxicity can be attributed to its presence on microglia and ability to mediate microglia-enhanced neurotoxicity, rather than a reduced sensitivity of DAergic neurons to MPP^+ due to MAC1-deficiency during development.

MAC1 is necessary for microglial activation elicited by MPP^+

To define the role of MAC1 expression in modulating microglial function, we first compared the morphological phenotype between $MAC1^{+/+}$ and $MAC1^{-/-}$ microglia in vitro in neuron-glia cultures with or without exposure to MPP^+. Activation of microglia was morphologically observed by F4/80 immunostaining at 1, 4, and 7 days after vehicle (media) or MPP^+ challenge. One day after treatment with 0.25 μM MPP^+, relatively few small and lightly stained microglia were observed in both $MAC1^{+/+}$ cultures and $MAC1^{-/-}$ cultures (Fig. 3*A*). Consistent with our previous report

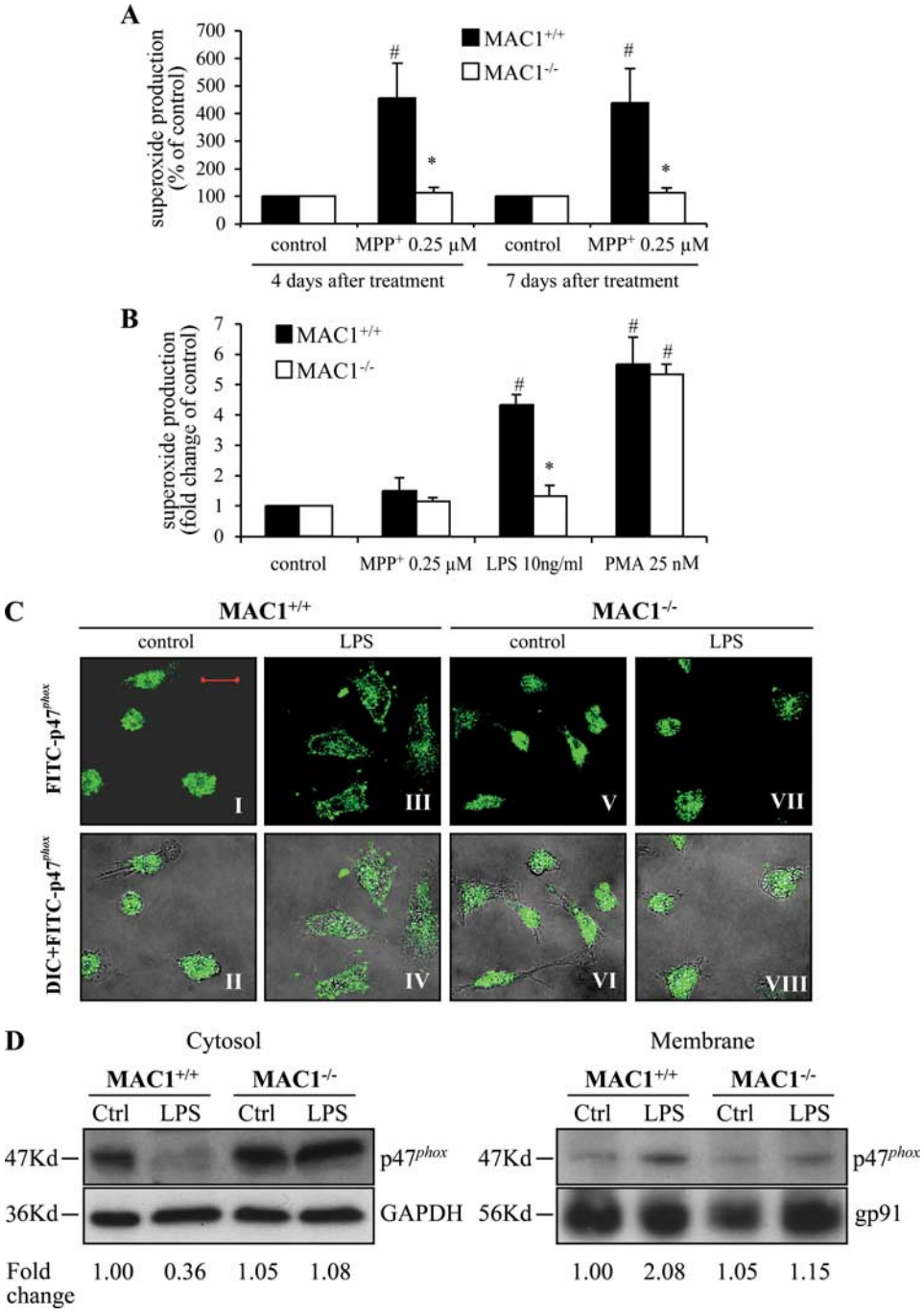

FIGURE 4. MAC1 mediates the activation of PHOX and production of superoxide. *A*, Mesencephalic neuron-glia cultures from MAC1$^{+/+}$ and MAC1$^{-/-}$ mice were treated with vehicle or MPP$^+$ (0.25 μM) for 4 or 7 days. *B*, Microglia-enriched cultures from MAC1$^{+/+}$ and MAC1$^{-/-}$ mice were treated with vehicle, PMA (25 nM), LPS (10 ng/ml), or MPP$^+$ (0.25 μM). Extracellular superoxide generation was measured by the SOD-inhibitable reduction of tetrazolium salt, WST-1. Data were mean ± SEM from three independent experiments in triplicates. #, $p < 0.05$ relative to corresponding vehicle-treated control cultures. *, $p < 0.05$ relative to MAC1$^{+/+}$ cultures after same treatments. *C*, Enriched microglial cells from MAC1$^{+/+}$ and MAC1$^{-/-}$ mice were treated with vehicle or LPS for 10 min. Cells were incubated with a rabbit polyclonal Ab against p47^{phox} and then with a FITC-conjugated goat anti-rabbit Ab. Focal planes spaced at 0.4 μm intervals were imaged. The signal of p47^{phox} (FITC-p47^{phox}; green) and the merged view of cell morphology and p47^{phox} (DIC plus FITC-p47^{phox}) were shown. Scale bar: 20 μm. *D*, Western blot assays for p47^{phox} levels in membrane and cytosolic fractions of microglia from MAC1$^{+/+}$ and MAC1$^{-/-}$ mice 10 min after vehicle or LPS treatment. Densitometry analysis was performed with values of p47^{phox} normalized to each respective loading control (GAPDH for cytosolic fraction, gp91 for membrane fraction) and further normalized to MAC1$^{+/+}$ controls. Experiments were performed at least three times.

(19), activation of microglia was prominent after prolonged MPP$^+$ treatment (4 and 7 days) in MAC1$^{+/+}$ cultures. Numerous activated microglia, characterized by intensified F4/80 staining and enlarged cell size, were distributed throughout the MAC1$^{+/+}$ cultures 4 days after MPP$^+$ exposure. At this time point, there was a mixture of process-bearing ramified microglia and process-free amoeboid-like microglia in MAC1$^{+/+}$ cultures. At 7 days posttreatment, more F4/80-positive cells in MAC1$^{+/+}$ cultures displayed features of fully activated microglia with an amoeboid and condensed morphology. In contrast, the MPP$^+$-induced activation of microglia was less pronounced in neuron-glia cultures from MAC1$^{-/-}$ mice at day 4 and day 7 posttreatment, exhibiting reduced F4/80 expression and minimal morphological changes. With vehicle treatment, there was no obvious morphological difference between MAC1$^{+/+}$ and MAC1$^{-/-}$ microglia. Western blot analysis using a different microglia marker (Iba1) was then performed to provide a quantitative estimation of microglial activation. Iba1 expression increased significantly 4 days after MPP$^+$ treatment in MAC1$^{+/+}$ cultures but not in MAC1$^{-/-}$ cultures (Fig. 3*B*). These results suggest that MAC1$^{-/-}$ microglia are less reactive compared with MAC1$^{+/+}$ microglia in the presence of MPP$^+$-induced neuronal damage.

MAC1 is critical for the activation of PHOX and subsequent oxidant production after MPP$^+$ treatment

To better characterize MAC1-mediated microglial activation and to further investigate the mechanisms underlying microglial MAC1-enhanced MPTP/MPP$^+$ neurotoxicity, we examined several factors released by microglia in cultures. Among the factors

we measured, the production of superoxide was the most prominently attenuated one in MAC1$^{-/-}$ cultures. The generation of extracellular superoxide was measured as SOD-inhibitable reduction of WST-1 in primary neuron-glia cultures following MPP$^+$ (0.25 μM) treatment. In MAC1$^{+/+}$ cultures, both 4 and 7 days of exposure of MPP$^+$ significantly stimulated the release of extracellular superoxide (Fig. 4*A*) compared with vehicle controls. In contrast, the production of superoxide after MPP$^+$ treatment was similar to control levels in MAC1$^{-/-}$ cultures, indicating the importance of MAC1 in the production of superoxide after prolonged MPP$^+$ treatment.

Because extracellular superoxide is an important factor mediating MAC1-enhanced MPP$^+$ neurotoxicity and PHOX is the key enzyme in extracellular superoxide generation in microglia, we further investigated whether PHOX activation was dependent upon MAC1 expression. First, to ensure the normal function of PHOX itself in MAC1$^{-/-}$ mice, microglia-enriched cultures from MAC1$^{+/+}$ and MAC1$^{-/-}$ mice were treated with vehicle, PMA, a potent protein kinase C agonist that can directly induce the production of superoxide catalyzed by PHOX, or LPS, an agent that triggers superoxide production via interacting with MAC1 (36; Fig. 4*B*). Although LPS induced significantly less production of superoxide in MAC1$^{-/-}$ microglia compared with that of MAC1$^{+/+}$ microglia, MAC1$^{+/+}$ and MAC1$^{-/-}$ microglia demonstrated the same capacity to produce superoxide after PMA, indicating an intact capability for PHOX-mediated superoxide production in these two genotypes. This suggests that the reduced production of superoxide observed in MAC1$^{-/-}$ neuron-glia cultures after MPP$^+$ exposure cannot be attributed to the malfunction of PHOX. It is noteworthy that no superoxide production was observed when MAC1$^{+/+}$ or MAC1$^{-/-}$ microglia were challenged by MPP$^+$, which confirms our previous report that MPP$^+$ cannot directly activate microglia in the absence of neuronal damage (19).

It is known that the activation of PHOX requires the translocation of cytoplasmic regulators (p47^{phox}, p67^{phox}, p40^{phox}, and Rac) and their subsequent interaction with the membrane-spanning flavocytochrome b558 to commence activation of superoxide production (37). To determine whether MAC1 regulates the translocation of cytosolic components of PHOX, the membrane translocation of p47^{phox} was monitored by measurement of cytosolic and membrane levels of p47^{phox} following activation of MAC1 by LPS. Microglia were labeled using anti-p47^{phox} Ab with FITC-conjugated secondary Ab. Using confocal microscopy, we observed a distinct morphological change in MAC1$^{+/+}$ microglia 10 min after LPS exposure, transforming from a small regular shape (Fig. 4*C*, *I* and *II*) into an irregularly enlarged shape (Fig. 4*C*, *III* and *IV*). Meanwhile, LPS increased the translocation of p47^{phox} from the cytosol (Fig. 4*C*, *I* and *II*) to the membrane (Fig. 4*C*, *III* and *IV*). The morphological change of microglia and translocation of p47^{phox} were absent in MAC1$^{-/-}$ microglia after LPS treatment (Fig. 4*C*, *VII* and *VIII*). Likewise, Western blot analyses showed a decrease in p47^{phox} levels in the cytosolic fraction of MAC1$^{+/+}$ microglia 10 min after LPS exposure (Fig. 4*D*). At the same time, membrane p47^{phox} expression levels increased. The membrane translocation of p47^{phox} was much less prominent in the MAC1$^{-/-}$ microglial fractions, consistent with the involvement of MAC1 activation in p47^{phox} membrane translocation.

MPP$^+$- induced PGE$_2$ production from microglia was reduced in MAC1-deficient mice

To further define the reactivity of MAC1$^{+/+}$ and MAC1$^{-/-}$ microglia to MPP$^+$-induced neuronal death, we measured the production of inflammatory factors including PGE$_2$, NO, TNF-α, and IL-1β. Because PGE$_2$ is produced by multiple types of CNS cells, a neuron-microglia coculture system was used to define the PGE$_2$ production from microglia induced by neuronal damage. MAC1$^{+/+}$ neuron-enriched culture, coculture of MAC1$^{+/+}$ neuron/MAC1$^{+/+}$ microglia, and coculture of MAC1$^{+/+}$ neuron/MAC1$^{-/-}$ microglia were treated with 0.25 μM MPP$^+$. The levels of released PGE$_2$ in supernatants were measured 4 days after treatment to determine whether MAC1 expression is important for microglial PGE$_2$ production in the presence of MPP$^+$-induced neuronal damage. After MPP$^+$ treatment PGE$_2$ production significantly increased in the cultures with microglia (MAC1$^{+/+}$ or MAC1$^{-/-}$), whereas it did not change in MAC1$^{+/+}$ neuron-enriched cultures (Fig. 5). Significantly reduced PGE$_2$ production was observed in MAC1$^{+/+}$ neuron and MAC1$^{-/-}$ microglia cocultures (37pg/ml) compared with that from cocultures of MAC1$^{+/+}$ neuron and MAC1$^{+/+}$ microglia (55pg/ml), suggesting the involvement of MAC1 in the microglial production of PGE$_2$.

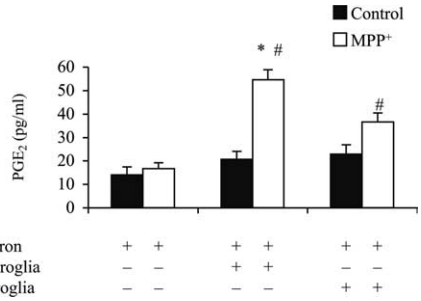

FIGURE 5. Involvement of MAC1 in MPP$^+$-induced PGE$_2$ production. Neuron-enriched cultures from MAC1$^{+/+}$ mice with or without microglia (MAC1$^{+/+}$ or MAC1$^{-/-}$) added back were compared for their ability to release PGE$_2$ into the culture medium. Microglia (1×10^5/well) were added back to MAC1$^{+/+}$ neuron-enriched cultures 24 h before treatment. Neuron-microglia cocultures were treated with vehicle or 0.25 μM MPP$^+$. Culture media were collected 4 days after treatment. Data were mean $\pm$ SEM from three independent experiments in triplicates. #, $p < 0.05$ relative to corresponding vehicle treated control cultures. *, $p < 0.05$ relative to cocultures of neuron and MAC1$^{-/-}$ microglia after same treatment.

NO, TNF-α, and IL-1β released by activated microglia were also measured in both MAC1$^{+/+}$ and MAC1$^{-/-}$ cultures treated with MPP$^+$. Their production was either below the detection limit after MPP$^+$ treatment or did not change significantly in MAC1 null mice vs wild type mice (data not shown).

MPTP-elicited DAergic neurotoxicity was attenuated in MAC1$^{-/-}$ mice in vivo

To recapitulate and substantiate the in vitro findings, MPTP (15 mg/kg) was injected s.c. to MAC1$^{+/+}$ and MAC1$^{-/-}$ mice for 6 consecutive days. We assessed the survival of DAergic neurons in the SNpc 21 days after the last injection through quantification of TH-positive neurons. MAC1$^{+/+}$ SNpc sections displayed decreased numbers of TH-positive neurons after MPTP treatment (Fig. 6*A*) compared with saline-injected controls (Fig. 6*B*). In contrast, MAC1$^{-/-}$ mice showed an attenuated loss of TH-positive neurons (Fig. 6, *C* and *D*). Quantitation of TH-positive neuron numbers by stereological assessment (Fig. 6*E*) confirmed the histological observations. There was a 47% survival of TH-positive neurons in MAC1$^{+/+}$ mice and 87% survival in the knockout mice after MPTP challenge, compared with the corresponding saline-injected controls, indicating that the loss of MAC1 confers resistance of SNpc DAergic neurons to MPTP-induced toxicity. No statistical difference was detected between saline-treated MAC1$^{+/+}$ and MAC1$^{-/-}$ mice in the number of TH-positive neurons in the SNpc.

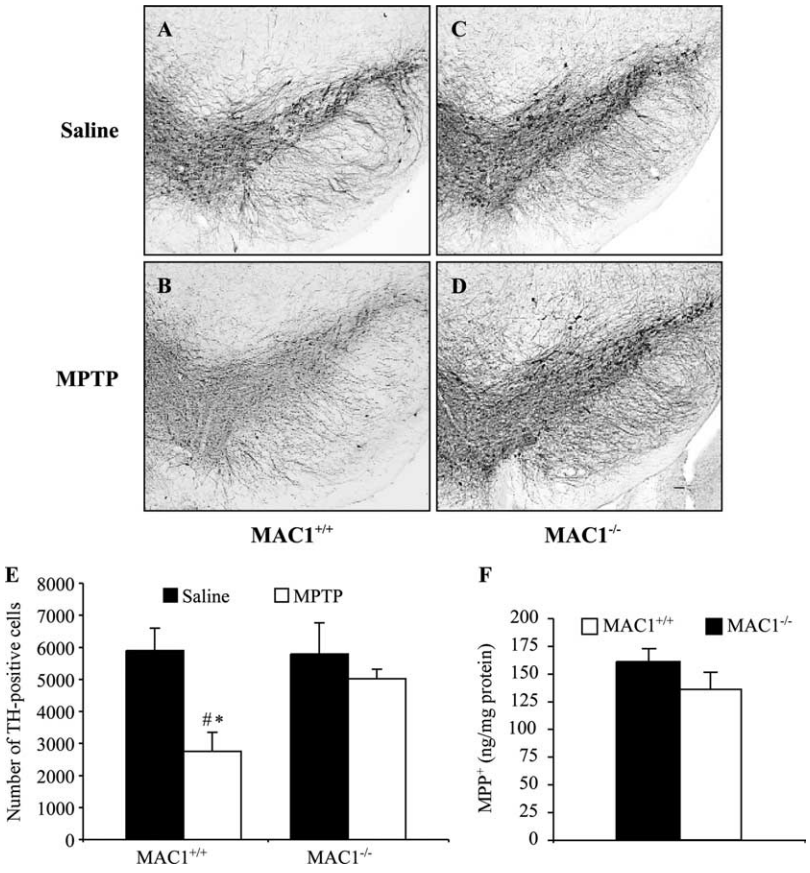

FIGURE 6. MPTP produced less DAergic neurotoxicity in MAC1$^{-/-}$ mice than MAC1$^{+/+}$ mice. MAC1$^{+/+}$ and MAC1$^{-/-}$ mice were injected s.c. with MPTP (15 mg/kg/day) or saline for 6 consecutive days. MPTP-mediated damage of DAergic neurons in SNpc was evaluated 21 days after the last injection by immunostaining with an Ab against TH. *A–D*, Immunostaining of TH-positive neurons in saline-treated (MAC1$^{+/+}$ (*A*); MAC1$^{-/-}$ (*C*)) and MPTP-treated (MAC1$^{+/+}$ (*B*); MAC1$^{-/-}$ (*D*)) mice. Scale bar: 50 μm. *E*, Quantification of SNpc TH-positive neurons in the mice in *A–D*. Results were presented as the mean ± SEM. Five to nine animals were used in each group. #, $p < 0.05$ compared with corresponding saline-treated controls. ∗, $p < 0.05$ compared with MAC1$^{-/-}$ mice after same treatment. *F*, HPLC determination of striatal MPP$^+$ levels in MAC1$^{+/+}$ and MAC1$^{-/-}$ mice 90 min after s.c. MPTP injection. Results were presented as the mean ± SEM. Three animals were used in each group.

DAergic neurons in SNpc send their axons into the striatum where they release DA at synapses on striatal neurons. Thus, we examined the striatal levels of DA and its metabolites (DOPAC and HVA) by HPLC at 21 days and 4 mo after MPTP injection. As shown in Table I, the levels of DA and its metabolites decreased significantly in MAC1$^{+/+}$ mice as compared with saline-injected controls at 21 days after MPTP injection. Interestingly, although a similar degree of striatal DA depletion (68%) was displayed in MAC1$^{-/-}$ mice at this time point, significantly higher levels of DOPAC and HVA were observed in MAC1$^{-/-}$ mice compared with MAC1$^{+/+}$ mice. The striatal DA level in MAC1$^{-/-}$ mice was restored to the control level 4 mo after MPTP administration, whereas significant reduction of DA and its metabolites still persisted in MAC1$^{+/+}$ mice. Brain levels of MPP$^+$ measured by HPLC showed no significant difference between MAC1$^{+/+}$ and MAC1$^{-/-}$ mice (Fig. 6*F*) 90 min following MPTP, indicating that the protection afforded by MAC1 deficiency was not due to an alteration in MPTP toxicokinetics.

MAC1 is necessary for reactive microgliosis elicited by MPTP in vivo

The morphological changes that accompany microglial activation after MPTP injection were examined in the SNpc. Microglia were stained with Iba1. Although resident microglia from both wild-type (Fig. 7*A*) and MAC1 null mice (Fig. 7*B*) express a basal level of Iba1, they appear small and bear thin processes (Fig. 7*A*, *inset*). Microglial activation, as demonstrated by a dramatic increase in Iba1 staining, was highly visible in the SNpc of the MAC1$^{+/+}$ mice at 7 days post-MPTP treatment (Fig. 7*C*). Numerous microglia assumed a highly activated amoeboid state with an enlarged cell body and thicker cellular processes (Fig. 7*C*, *inset*) compared

Table I. *Striatal levels (ng/100mg wet sample) of DA and its metabolites at 21 days and 4 mo after the last MPTP injection*[a]

	21 days				4 mo			
	DA	DOPAC	HVA	Turnover[b]	DA	DOPAC	HVA	Turnover[b]
Saline[c]	963.10 ± 16.85	97.312 ± 15.14	100.53 ± 16.22	0.21 ± 0.03	1032.04 ± 32.28	97.22 ± 8.04	112.97 ± 11.59	0.20 ± 0.01
MPTP								
MAC1$^{+/+}$	304.07 ± 8.16[d]	30.70 ± 2.67[e]	53.2 ± 1.45[e]	0.28 ± 0.01	518.23 ± 86.55[e]	72.39 ± 2.88[d]	71.82 ± 10.13[e]	0.29 ± 0.04
MAC1$^{-/-}$	310.23 ± 17.54[d]	139.77 ± 21.86	84.26 ± 4.23	0.72 ± 0.04[f]	1007.24 ± 63.09	83.74 ± 6.13	100.81 ± 9.07	0.18 ± 0.01

[a] MAC1$^{+/+}$ or MAC1$^{-/-}$ mice were injected with vehicle (saline) or MPTP as described in *Materials and Methods*. Mice were sacrificed and striatal tissues were removed 21 days or 4 mo after the last MPTP injection. The levels of DA and its metabolites, DOPAC and HVA, were determined with HPLC and expressed as means ± SEM. Three to six animals were used in each group.

[b] Turnover ratio = (DOPAC + HVA)/DA. This ratio is often used to reflect the activity of DAergic neurons.

[c] As DA, DOPAC, and HVA values were not different between saline-injected MAC1$^{+/+}$ or MAC1$^{-/-}$ mice, data from both groups were combined.

[d] $p < 0.05$, different from saline-injected control mice.

[e] $p < 0.05$, different from saline-injected control mice and MPTP-injected MAC1$^{-/-}$ mice.

[f] $p < 0.05$, different from saline-injected control mice and MPTP-injected MAC1$^{+/+}$ mice.

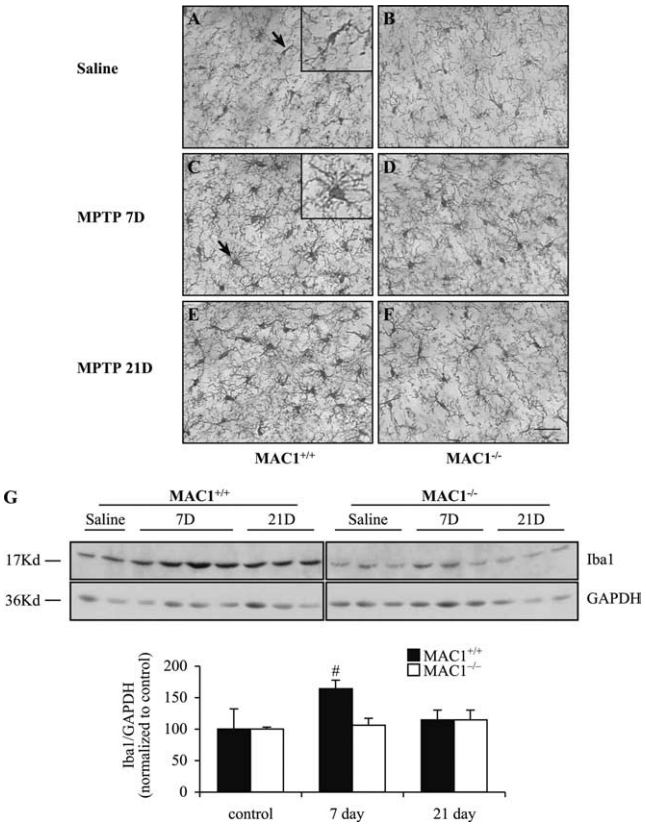

FIGURE 7. Analysis of MPTP-induced reactive microgliosis in vivo. $MAC1^{+/+}$ and $MAC1^{-/-}$ mice were sacrificed 7 days and 21 days following saline or MPTP s.c. injection. *A–F*, Brain sections were immunostained with an Iba1 Ab specific for microglia. Magnified images of resting (arrow in *A*) and activated microglia (arrow in *C*) were shown in the insets. The images were representative of three to four animals per group. Scale bar: 50 μm (*inset*: 25 μm). *G*, Western blot results with detection of Iba1 in midbrain tissue extracts from $MAC1^{+/+}$ and $MAC1^{-/-}$ mice. GAPDH was used as loading control. The ratio of densitometry values of Iba1 and GAPDH was analyzed and normalized to each respective control. Results were presented as the mean ± SEM. #, $p < 0.05$ relative to corresponding vehicle-treated control.

with those in saline-injected control animals. At 21 days post-MPTP treatment, the activation of microglia subsided but was still observed (Fig. 7*E*) in $MAC1^{+/+}$ mice. In contrast, microglial activation in the $MAC1^{-/-}$ mice following MPTP (Fig. 7, *D* and *F*) was not significantly changed from the controls. Western blot analysis of whole tissue extracts from midbrain 7 days after MPTP treatment demonstrated a marked increase in Iba1 expression in the $MAC1^{+/+}$ mice (Fig. 7*G*) but not in $MAC1^{-/-}$ mice, which corroborates well with immunohistochemistry data.

Discussion

In this study the critical role of MAC1 in reactive microgliosis and DAergic neurodegeneration was demonstrated by the findings that MAC1 deficiency greatly attenuated the microglial activation and DAergic neurodegeneration induced by MPTP or MPP^+ exposure both in vivo and in vitro, respectively. Mechanistic studies revealed that significantly reduced release of superoxide and PGE_2 may underlie the attenuated neurotoxicity in MAC1-deficient neuron-glia cultures. Furthermore, the failure of superoxide production and $p47^{phox}$ membrane translocation in $MAC1^{-/-}$ microglia strongly suggests a close coupling between MAC1 and PHOX activation.

The elevated expression of MAC1, a β_2 integrin family member that is expressed exclusively on microglia in the CNS, has been reported in the postmortem brains of patients with Alzheimer's disease (27) and in the MPTP model of PD (16), suggesting a possible role for this receptor in neurodegeneration. In the current study we revealed that MAC1 deficiency mitigated the loss of DAergic neurons, both in vitro (Fig. 1) and in vivo (Fig. 6), induced by MPP^+/MPTP exposure. These results prove that MAC1 is critical in the MPTP neurotoxic process. MAC1 deficiency did not change the sensitivity of neurons per se because MPP^+ exerted the same degree of toxicity in neuron-enriched cultures from $MAC1^{-/-}$ and $MAC1^{+/+}$ mice (Fig. 2*A*). In contrast, the presence of microglia with functional MAC1 expression was essential for the differential sensitivity to MPP^+ neurotoxicity in $MAC1^{-/-}$ and $MAC1^{+/+}$ neuron-glia cultures (Fig. 2, *B* and *C*). Lack of MAC1 expression was also not associated with alteration in the formation of MPP^+ (Fig. 6*F*). Therefore, the resistance of MAC1-deficient mice to MPTP/MPP^+ results from the absence of MAC1 on microglia, and not from either an alteration in the response of DAergic neurons to the toxin or an impaired MPTP metabolism. This conclusion was further supported by the lack of a robust, persistent reactive microgliosis in mesencephalic cultures (Fig. 3) or SNpc (Fig. 7) from $MAC1^{-/-}$ mice following MPP^+ or MPTP, respectively. Together with previous reports showing the indispensable role of neuronal damage for microglial activation following MPTP (19, 38), these data indicate a compromised neuron-microglial cross-talk in $MAC1^{-/-}$ mice. Thus, this study highlights the critical role of MAC1 in the activation of microglia induced by neuronal damage and subsequent microglia-enhanced neurotoxicity.

The importance of MAC1 in microglial activation is not likely restricted to the MPTP model of PD. For example, β-amyloid has been observed to mediate release of NO from cultured microglia via its binding to MAC1 (39), suggesting a possible association between MAC1 and Alzheimer's disease. Recent evidence also indicates that MAC1 mediates the differentiation of microglia to phagocytes in inflammatory demyelinating disease via the interaction with fibrinogen, which is deposited perivascularly in multiple sclerosis plaques (20).

An interesting unresolved question is that of the exact mechanism by which MAC1 is activated in the presence of damaged neurons. Soluble factors released from injured neurons might be ligands for MAC1. For instance, α-synuclein, a presynaptic protein involved in PD, activates microglia via interaction with MAC1 (40). Injured neurons also release proteases, such as matrix metalloproteinase-3 (41), causing extracellular matrix (ECM) degradation. The degraded ECM molecules may activate MAC1. Additionally, MAC1 might also be activated via direct cell-cell contact with damaged neurons. Significantly increased contacts between microglial processes and neurons after the neuronal injury has been quantitatively demonstrated (42). Indeed, MAC1 is known to be the most promiscuous integrin that interacts actively with diverse endogenous ligands (43) such as ECM proteins, the counterreceptor intracellular adhesion molecule-1 (ICAM, CD54; Ref. 44) and complement iC3b (45). In this regard, all the above mentioned pathways may be involved and may work together to trigger microglial activation via interactions with MAC1. In what appears to be consistent with this assumption, a previous report demonstrated that both direct contact and neuron-released factors contribute to the activation of microglia after MPP^+ treatment (46).

Activated microglia exert cytotoxic effects by releasing excessive amounts of inflammatory mediators, such as free radicals, proinflammatory factors, and arachidonic acid derivatives (10). Consistent with our previous report (19), we demonstrated here that superoxide is a prominent microglia-released factor following MPTP/MPP^+ exposure. Although MPP^+ cannot stimulate the production of superoxide directly from enriched microglia (Fig. 4*B*),

it induces a significantly increased production of superoxide in neuron-glia mixed cultures (Fig. 4*A*), where microglia were activated secondary to MPP^+-induced neuronal damage (19). The present study advances our understanding of the mechanism of superoxide production following MPP^+-induced neuronal injury. We observed substantially attenuated superoxide production in neuron-glia cultures isolated from $MAC1^{-/-}$ mice as compared with that from respective $MAC1^{+/+}$ mice (Fig. 4*A*), suggesting that MAC1 is a key receptor for damaged neuron-derived signals to activate microglia and to induce extracellular superoxide production. In fact, it has been shown that MAC1 engagement is important in mediating the peripheral polymorphonuclear cells burst of superoxide anion (47–49). Recent reports from our group indicate that MAC1 is a potential receptor mediating microglial activation and the production of extracellular superoxide after LPS (36) and α-synuclein (40) insults. In conjugation with our observations here, MAC1 seems to be an indispensable receptor for the production of superoxide in microglia in response to multiple external stimulants.

We further demonstrated that MAC1 affects the production of superoxide by regulating the activity of PHOX. The role of microglial MAC1 in PHOX activation is supported by our results demonstrating translocation of $p47^{phox}$ from cytosol to cell membrane in $MAC1^{+/+}$ cultures but not in $MAC1^{-/-}$ cultures after treatment with a known ligand of MAC1 (Fig. 4, *C* and *D*). This conclusion is consistent with earlier reports of MAC1-mediated PHOX activation in neutrophils (21, 49) and eosinophils (22). Existing evidence shows that functional PHOX is expressed not only by microglia but also by astroglia (50), another major type of glial cell in the CNS. It suggests the possibility that astroglia might also be the source of superoxide production after MPP^+ treatment. However, our previous results (19) indicate that microglia, but not astroglia, dictated an enhanced sensitivity of DAergic neurons to MPP^+ neurotoxicity. Therefore, it seems that the production of superoxide from astroglia after MPP^+ exposure is minimal and may not be sufficient to elicit neurotoxicity.

PGE_2 production and COX-2 expression in microglia has been previously proposed to be important for MPTP/MPP^+-induced DAergic neurotoxicity (51). COX-2 deficiency or specific inhibition attenuated MPTP/MPP^+-induced degeneration of TH-positive cells (52, 53). In this study, we demonstrated that the production of PGE_2 increased significantly after MPP^+ treatment in neuron-microglia cocultures but not in neuron-enriched cultures (Fig. 5). We further found that microglial deficiency of MAC1 significantly reduced, but did not abolish, the production of PGE_2 in neuron-microglia cocultures. These results are consistent with the view that MAC1 functions in concert with other receptors or molecules to induce the production of PGE_2 in microglia. Interestingly, for other inflammatory cytokines (TNF-α and IL-1β) we tested by real time PCR or ELISA (data not shown), there is no significant difference between $MAC1^{-/-}$ and $MAC1^{+/+}$ cultures. In what appears to be consistent with our findings here, Perera et al. reported (54) that MAC1 plays a significant role in the optimal production of some genes (such as COX-2), whereas it is not necessary for the expression of other genes (such as TNF-α) induced by Taxol or LPS in microphages.

It is important to note that in our in vivo experiments, the sparing of the SNpc DAergic neurons observed 21 days after MPTP injection (Fig. 6) in $MAC1^{-/-}$ mice was not accompanied by a similar protection of striatal DA levels (Table I). The preservation of striatal DA levels was only observed at a much later time point (4 mo, Table I) in $MAC1^{-/-}$ mice. We speculate that the above-mentioned disparity is due to the fact that different mechanisms are involved in causing the loss of SNpc DAergic neurons and the decrease in striatal DA levels. Initially, MPTP directly induces a rapid and drastic depletion of DA in striatal DAergic fibers (55, 56), resulting in a similar striatal DA depletion in $MAC1^{-/-}$ and $MAC1^{+/+}$ mice. In contrast, MPTP-induced degeneration of SNpc DAergic neuronal cell bodies involved the participation of microglia, where MAC1 plays a critical role leading to the microglial activation. Although the degree of striatal DA loss in $MAC1^{-/-}$ mice was the same as that in $MAC1^{+/+}$ mice 21 days following MPTP, the increased turnover of DA, as characterized by increased ($DOPAC^+HVA$)/DA ratio, was observed (Table I) in $MAC1^{-/-}$ mice. Among various possibilities, this result may reflect a better preserved DAergic neuronal function with compensatory increased DA synthesis and release (56) in $MAC1^{-/-}$ mice, which in turn led to a speedier restoration of striatal DA levels than the wild-type mice as observed at 4 mo after MPTP injection (Table I). Similarly, the unparalleled recovery of striatal DA levels with the preservation of the SNpc DAergic neurons has also been observed after the administration of several neuroprotective drugs or genetic manipulations (16, 55).

Although the existence of persistent reactive microgliosis has been recognized in many neurodegenerative diseases including PD (57), Alzheimer's disease (58), multiple sclerosis (59), and Huntington's disease (60), lack of understanding of the specific mechanisms initiating activation of microglia has hampered development of new therapeutic approaches targeting microgliosis. This study demonstrates that MAC1 contributes to the MPTP/MPP^+-induced reactive microgliosis and progressive DAergic neurodegeneration. In this paradigm, PHOX-generated superoxide and PGE_2 are two important cytotoxic factors regulated by MAC1. Our study provides insights into the mechanism by which damaged neurons activate microglia and thus set in motion a self-perpetuating cycle of neuronal death and microglial activation. In this regard, strategies aimed at inhibiting MAC1 may provide a novel microglia-suppressive therapy for the treatment of PD and other neurodegenerative diseases.

Acknowledgments

We thank Anthony Lockhart for assistance with animal colony management and maintenance of the timed pregnant mice. We are grateful to Dr. Song-Jen Wei, Dr. Hung-ming Wu, and Dr. Hui-ling Chen at National Institute of Environmental Health Sciences for technical assistance.

Disclosures

The authors have no financial conflict of interest.

References

1. Leenders, K. L., and W. H. Oertel. 2001. Parkinson's disease: clinical signs and symptoms, neural mechanisms, positron emission tomography, and therapeutic interventions. *Neural Plast.* 8: 99–110.
2. Kreutzberg, G. W. 1996. Microglia: a sensor for pathological events in the CNS. *Trends Neurosci* 19: 312–318.
3. Gao, H. M., and J. S. Hong. 2008. Why neurodegenerative diseases are progressive: uncontrolled inflammation drives disease progression. *Trends Immunol.* 29: 357–365.
4. McGeer, P. L., S. Itagaki, B. E. Boyes, and E. G. McGeer. 1988. Reactive microglia are positive for HLA-DR in the substantia nigra of Parkinson's and Alzheimer's disease brains. *Neurology* 38: 1285–1291.
5. Benveniste, E. N., V. T. Nguyen, and G. M. O'Keefe. 2001. Immunological aspects of microglia: relevance to Alzheimer's disease. *Neurochem. Int.* 39: 381–391.
6. Yrjanheikki, J., R. Keinanen, M. Pellikka, T. Hokfelt, and J. Koistinaho. 1998. Tetracyclines inhibit microglial activation and are neuroprotective in global brain ischemia. *Proc. Natl. Acad. Sci. USA* 95: 15769–15774.
7. Nakamura, Y. 2002. Regulating factors for microglial activation. *Biol. Pharm. Bull.* 25: 945–953.
8. Aloisi, F. 1999. The role of microglia and astrocytes in CNS immune surveillance and immunopathology. *Adv. Exp. Med. Biol.* 468: 123–133.
9. Batchelor, P. E., G. T. Liberatore, J. Y. Wong, M. J. Porritt, F. Frerichs, G. A. Donnan, and D. W. Howells. 1999. Activated macrophages and microglia induce dopaminergic sprouting in the injured striatum and express brain-derived neurotrophic factor and glial cell line-derived neurotrophic factor. *J. Neurosci.* 19: 1708–1716.

10. Liu, B., and J. S. Hong. 2003. Role of microglia in inflammation-mediated neurodegenerative diseases: mechanisms and strategies for therapeutic intervention. *J. Pharmacol. Exp. Ther.* 304: 1–7.
11. Block, M. L., L. Zecca, and J. S. Hong. 2007. Microglia-mediated neurotoxicity: uncovering the molecular mechanisms. *Nat. Rev. Neurosci.* 8: 57–69.
12. Langston, J. W., P. Ballard, J. W. Tetrud, and I. Irwin. 1983. Chronic Parkinsonism in humans due to a product of meperidine-analog synthesis. *Science* 219: 979–980.
13. Langston, J. W., and I. Irwin. 1986. MPTP: current concepts and controversies. *Clin. Neuropharmacol.* 9: 485–507.
14. Langston, J. W., L. S. Forno, J. Tetrud, A. G. Reeves, J. A. Kaplan, and D. Karluk. 1999. Evidence of active nerve cell degeneration in the substantia nigra of humans years after 1-methyl-4-phenyl-1,2,3,6-tetrahydropyridine exposure. *Ann. Neurol.* 46: 598–605.
15. McGeer, P. L., C. Schwab, A. Parent, and D. Doudet. 2003. Presence of reactive microglia in monkey substantia nigra years after 1-methyl-4-phenyl-1,2,3,6-tetrahydropyridine administration. *Ann. Neurol.* 54: 599–604.
16. Liberatore, G. T., V. Jackson-Lewis, S. Vukosavic, A. S. Mandir, M. Vila, W. G. McAuliffe, V. L. Dawson, T. M. Dawson, and S. Przedborski. 1999. Inducible nitric oxide synthase stimulates dopaminergic neurodegeneration in the MPTP model of Parkinson disease. *Nat. Med.* 5: 1403–1409.
17. Jackson-Lewis, V., M. Jakowec, R. E. Burke, and S. Przedborski. 1995. Time course and morphology of dopaminergic neuronal death caused by the neurotoxin 1-methyl-4-phenyl-1,2,3,6-tetrahydropyridine. *Neurodegeneration* 4: 257–269.
18. Wu, D. C., V. Jackson-Lewis, M. Vila, K. Tieu, P. Teismann, C. Vadseth, D. K. Choi, H. Ischiropoulos, and S. Przedborski. 2002. Blockade of microglial activation is neuroprotective in the 1-methyl-4-phenyl-1,2,3,6-tetrahydropyridine mouse model of Parkinson disease. *J. Neurosci.* 22: 1763–1771.
19. Gao, H. M., B. Liu, W. Zhang, and J. S. Hong. 2003. Critical role of microglial NADPH oxidase-derived free radicals in the in vitro MPTP model of Parkinson's disease. *FASEB J.* 17: 1954–1956.
20. Adams, R. A., J. Bauer, M. J. Flick, S. L. Sikorski, T. Nuriel, H. Lassmann, J. L. Degen, and K. Akassoglou. 2007. The fibrin-derived γ377–395 peptide inhibits microglia activation and suppresses relapsing paralysis in central nervous system autoimmune disease. *J. Exp. Med.* 204: 571–582.
21. Mayadas, T. N., and X. Cullere. 2005. Neutrophil β2 integrins: moderators of life or death decisions. *Trends Immunol.* 26: 388–395.
22. Lynch, O. T., M. A. Giembycz, P. J. Barnes, P. G. Hellewell, and M. A. Lindsay. 1999. "Outside-in" signalling mechanisms underlying CD11b/CD18-mediated NADPH oxidase activation in human adherent blood eosinophils. *Br. J. Pharmacol.* 128: 1149–1158.
23. Coxon, A., P. Rieu, F. J. Barkalow, S. Askari, A. H. Sharpe, U. H. von Andrian, M. A. Arnaout, and T. N. Mayadas. 1996. A novel role for the β 2 integrin CD11b/CD18 in neutrophil apoptosis: a homeostatic mechanism in inflammation. *Immunity* 5: 653–666.
24. Le Cabec, V., S. Carreno, A. Moisand, C. Bordier, and I. Maridonneau-Parini. 2002. Complement receptor 3 (CD11b/CD18) mediates type I and type II phagocytosis during nonopsonic and opsonic phagocytosis, respectively. *J. Immunol.* 169: 2003–2009.
25. Ingalls, R. R., M. A. Arnaout, R. L. Delude, S. Flaherty, R. Savedra, Jr., and D. T. Golenbock. 1998. The CD11/CD18 integrins: characterization of three novel LPS signaling receptors. *Prog. Clin. Biol. Res.* 397: 107–117.
26. Medvedev, A. E., T. Flo, R. R. Ingalls, D. T. Golenbock, G. Teti, S. N. Vogel, and T. Espevik. 1998. Involvement of CD14 and complement receptors CR3 and CR4 in nuclear factor-κB activation and TNF production induced by lipopolysaccharide and group B streptococcal cell walls. *J. Immunol.* 160: 4535–4542.
27. Akiyama, H., and P. L. McGeer. 1990. Brain microglia constitutively express β-2 integrins. *J. Neuroimmunol.* 30: 81–93.
28. Gao, H. M., J. S. Hong, W. Zhang, and B. Liu. 2002. Distinct role for microglia in rotenone-induced degeneration of dopaminergic neurons. *J. Neurosci.* 22: 782–790.
29. Zhang, W., E. J. Shin, T. Wang, P. H. Lee, H. Pang, M. B. Wie, W. K. Kim, S. J. Kim, W. H. Huang, Y. Wang, et al. 2006. 3-Hydroxymorphinan, a metabolite of dextromethorphan, protects nigrostriatal pathway against MPTP-elicited damage both in vivo and in vitro. *FASEB J.* 20: 2496–2511.
30. McCormack, A. L., M. Thiruchelvam, A. B. Manning-Bog, C. Thiffault, J. W. Langston, D. A. Cory-Slechta, and D. A. Di Monte. 2002. Environmental risk factors and Parkinson's disease: selective degeneration of nigral dopaminergic neurons caused by the herbicide paraquat. *Neurobiol. Dis.* 10: 119–127.
31. Caudle, W. M., J. R. Richardson, M. Z. Wang, T. N. Taylor, T. S. Guillot, A. L. McCormack, R. E. Colebrooke, D. A. Di Monte, P. C. Emson, and G. W. Miller. 2007. Reduced vesicular storage of dopamine causes progressive nigrostriatal neurodegeneration. *J. Neurosci.* 27: 8138–8148.
32. West, M. J., L. Slomianka, and H. J. Gundersen. 1991. Unbiased stereological estimation of the total number of neurons in thesubdivisions of the rat hippocampus using the optical fractionator. *Anat. Rec.* 231: 482–497.
33. Chan, P., D. A. Di Monte, J. W. Langston, and A. M. Janson. 1997. $^{+}$MK-801 does not prevent MPTP-induced loss of nigral neurons in mice. *J. Pharmacol. Exp. Ther.* 280: 439–446.
34. Ali, S. F., S. N. David, G. D. Newport, J. L. Cadet, and W. Slikker, Jr. 1994. MPTP-induced oxidative stress and neurotoxicity are age-dependent: evidence from measures of reactive oxygen species and striatal dopamine levels. *Synapse* 18: 27–34.
35. Qian, L., K. S. Tan, S. J. Wei, H. M. Wu, Z. Xu, B. Wilson, R. B. Lu, J. S. Hong, and P. M. Flood. 2007. Microglia-mediated neurotoxicity is inhibited by morphine through an opioid receptor-independent reduction of NADPH oxidase activity. *J. Immunol.* 179: 1198–1209.
36. Pei, Z., H. Pang, L. Qian, S. Yang, T. Wang, W. Zhang, X. Wu, S. Dallas, B. Wilson, J. M. Reece, et al. 2007. MAC1 mediates LPS-induced production of superoxide by microglia: the role of pattern recognition receptors in dopaminergic neurotoxicity. *Glia* 55: 1362–1373.
37. Babior, B. M. 1999. NADPH oxidase: an update. *Blood* 93: 1464–1476.
38. Wu, D. C., P. Teismann, K. Tieu, M. Vila, V. Jackson-Lewis, H. Ischiropoulos, and S. Przedborski. 2003. NADPH oxidase mediates oxidative stress in the 1-methyl-4-phenyl-1,2,3,6-tetrahydropyridine model of Parkinson's disease. *Proc. Natl. Acad. Sci. USA* 100: 6145–6150.
39. Goodwin, J. L., M. E. Kehrli, Jr., and E. Uemura. 1997. Integrin Mac-1 and β-amyloid in microglial release of nitric oxide. *Brain Res.* 768: 279–286.
40. Zhang, W., S. Dallas, D. Zhang, J. P. Guo, H. Pang, B. Wilson, D. S. Miller, B. Chen, W. Zhang, P. L. McGeer, et al. 2007. Microglial PHOX and Mac-1 are essential to the enhanced dopaminergic neurodegeneration elicited by A30P and A53T mutant α-synuclein. *Glia* 55: 1178–1188.
41. Kim, Y. S., S. S. Kim, J. J. Cho, D. H. Choi, O. Hwang, D. H. Shin, H. S. Chun, M. F. Beal, and T. H. Joh. 2005. Matrix metalloproteinase-3: a novel signaling proteinase from apoptotic neuronal cells that activates microglia. *J. Neurosci.* 25: 3701–3711.
42. Hasegawa, S., M. Yamaguchi, H. Nagao, M. Mishina, and K. Mori. 2007. Enhanced cell-to-cell contacts between activated microglia and pyramidal cell dendrites following kainic acid-induced neurotoxicity in the hippocampus. *J. Neuroimmunol.* 186: 75–85.
43. Ehlers, M. R. 2000. CR3: a general purpose adhesion-recognition receptor essential for innate immunity. *Microbes Infect.* 2: 289–294.
44. Diamond, M. S., D. E. Staunton, A. R. de Fougerolles, S. A. Stacker, J. Garcia-Aguilar, M. L. Hibbs, and T. A. Springer. 1990. ICAM-1 (CD54): a counter-receptor for Mac-1 (CD11b/CD18). *J. Cell Biol.* 111: 3129–3139.
45. Dana, N., D. M. Fathallah, and M. A. Arnaout. 1991. Expression of a soluble and functional form of the human β 2 integrin CD11b/CD18. *Proc. Natl. Acad. Sci. USA* 88: 3106–3110.
46. Zhou, Y., Y. Wang, M. Kovacs, J. Jin, and J. Zhang. 2005. Microglial activation induced by neurodegeneration: a proteomic analysis. *Mol. Cell. Proteomics* 4: 1471–1479.
47. Vaporciyan, A. A., and P. A. Ward. 1993. Enhanced generation of O2- by human neutrophils via a complement iC3b/Mac-1 interaction. *Biol. Signals* 2: 126–135.
48. Dapino, P., F. Dallegri, L. Ottonello, and C. Sacchetti. 1993. Induction of neutrophil respiratory burst by tumour necrosis factor-α; priming effect of solid-phase fibronectin and intervention of CD11b-CD18 integrins. *Clin. Exp. Immunol.* 94: 533–538.
49. Gao, X. P., X. Zhu, J. Fu, Q. Liu, R. S. Frey, and A. B. Malik. 2007. Blockade of class IA phosphoinositide 3-kinase in neutrophils prevents NADPH oxidase activation- and adhesion-dependent inflammation. *J. Biol. Chem.* 282: 6116–6125.
50. Abramov, A. Y., and M. R. Duchen. 2005. The role of an astrocytic NADPH oxidase in the neurotoxicity of amyloid β peptides. *Philos. Trans. R. Soc. Lond. B Biol. Sci.* 360: 2309–2314.
51. Wang, X., C. L. Shen, M. T. Dyson, S. Eimerl, J. Orly, J. C. Hutson, and D. M. Stocco. 2005. Cyclooxygenase-2 regulation of the age-related decline in testosterone biosynthesis. *Endocrinology* 146: 4202–4208.
52. Vijitruth, R., M. Liu, D. Y. Choi, X. V. Nguyen, R. L. Hunter, and G. Bing. 2006. Cyclooxygenase-2 mediates microglial activation and secondary dopaminergic cell death in the mouse MPTP model of Parkinson's disease. *J. Neuroinflammation* 3: 6.
53. Feng, Z. H., T. G. Wang, D. D. Li, P. Fung, B. C. Wilson, B. Liu, S. F. Ali, R. Langenbach, and J. S. Hong. 2002. Cyclooxygenase-2-deficient mice are resistant to 1-methyl-4-phenyl1, 2, 3, 6-tetrahydropyridine-induced damage of dopaminergic neurons in the substantia nigra. *Neurosci. Lett.* 329: 354–358.
54. Perera, P. Y., T. N. Mayadas, O. Takeuchi, S. Akira, M. Zaks-Zilberman, S. M. Goyert, and S. N. Vogel. 2001. CD11b/CD18 acts in concert with CD14 and Toll-like receptor (TLR) 4 to elicit full lipopolysaccharide and taxol-inducible gene expression. *J. Immunol.* 166: 574–581.
55. Zhang, W., T. Wang, L. Qin, H. M. Gao, B. Wilson, S. F. Ali, W. Zhang, J. S. Hong, and B. Liu. 2004. Neuroprotective effect of dextromethorphan in the MPTP Parkinson's disease model: role of NADPH oxidase. *FASEB J.* 18: 589–591.
56. Leng, A., A. Mura, B. Hengerer, J. Feldon, and B. Ferger. 2004. Effects of blocking the dopamine biosynthesis and of neurotoxic dopamine depletion with 1-methyl-4-phenyl-1,2,3,6-tetrahydropyridine (MPTP) on voluntary wheel running in mice. *Behav. Brain Res.* 154: 375–383.
57. Imamura, K., N. Hishikawa, M. Sawada, T. Nagatsu, M. Yoshida, and Y. Hashizume. 2003. Distribution of major histocompatibility complex class II-positive microglia and cytokine profile of Parkinson's disease brains. *Acta Neuropathol.* 106: 518–526.
58. McGeer, P. L., S. Itagaki, H. Tago, and E. G. McGeer. 1987. Reactive microglia in patients with senile dementia of the Alzheimer type are positive for the histocompatibility glycoprotein HLA-DR. *Neurosci. Lett.* 79: 195–200.
59. Takeuchi, H., J. Wang, J. Kawanokuchi, N. Mitsuma, T. Mizuno, and A. Suzumura. 2006. Interferon-γ induces microglial-activation-induced cell death: a hypothetical mechanism of relapse and remission in multiple sclerosis. *Neurobiol. Dis.* 22: 33–39.
60. Sapp, E., K. B. Kegel, N. Aronin, T. Hashikawa, Y. Uchiyama, K. Tohyama, P. G. Bhide, J. P. Vonsattel, and M. DiFiglia. 2001. Early and progressive accumulation of reactive microglia in the Huntington disease brain. *J. Neuropathol. Exp. Neurol.* 60: 161–172.